Probing the Nature of Surface Hydrides by Deuterium Quadrupolar Parameters: A Case Study on Silica-Supported Zirconium Hydrides

Journal Article

Author(s):
Docherty, Scott R.; Schärz, Philipp; Gioffrè, Domenico; Yakimov, Alexander; Copéret, Christophe

Publication date:
2024-01

Permanent link:
https://doi.org/10.3929/ethz-b-000648546

Originally published in:
Helvetica Chimica Acta 107(1), https://doi.org/10.1002/hlca.202300173

Funding acknowledgement:
169134 - Molecular Approach to Heterogeneous Catalysis (SNF)
192050 - Molecular Approach and Understanding in Heterogeneous Catalysis (SNF)

doi.org/10.1002/hlca.202300173

RESEARCH ARTICLE

HELVETICA chimica acta

Probing the Nature of Surface Hydrides by Deuterium Quadrupolar Parameters: A Case Study on Silica-Supported Zirconium Hydrides

Scott R. Docherty,[a] Philipp Schärz,[a] Domenico Gioffrè,[a] Alexander V. Yakimov,[a] and Christophe Copéret*[a]

[a] Department of Chemistry and Applied Biosciences, ETH Zürich, Vladimir Prelog Weg 1–5, CH-8093 Zurich, Switzerland, e-mail: ccoperet@inorg.chem.ethz.ch

Dedicated to *Scott Denmark* on the occasion of his 70th birthday

Supported metal hydrides are key reactive intermediates in various catalytic processes, such as hydrogenation and dehydrogenation, but are often challenging to characterize spectroscopically. Here, deuterium solid state nuclear magnetic resonance spectroscopy is used to understand the structure of the corresponding silica-supported zirconium hydrides after H/D exchange as an illustrative example of supported metal hydrides, which have been shown to display notable reactivity towards small molecules (*e.g.*, CO_2 and N_2O) and to activate both C–H and C–C bonds, hence their use in to the conversion of hydrocarbons (alkanes, polyolefins *etc.*)

Keywords: H/D exchange, hydrides, metal hydrides, solid-state NMR, solid-state structures.

Introduction

Supported transition-metal hydrides (M–H) are key intermediates in hydrocarbon conversion processes, such as hydrogenation and dehydrogenation.[1,2] When isolated on an oxide support, early transition metal hydrides participate in low temperature hydrogenolysis and alkane metathesis processes, which involve C–H and C–C activation (through σ-bond metathesis), as key (elementary) steps.[1–5] In particular, these early transition metal hydrides, such as supported Zr hydrides,[6–8] have attracted a renewed interest in recent years in the context of polyolefin reprocessing as they are known to activate C–H bonds and to participate in the conversion of polyethylene into diesel or lower range hydrocarbons.[8–11]

While key intermediates for these reactions, M–H bonds are often challenging to characterize spectroscopically in heterogeneous catalysts due to various experimental limitations.[1] For example, Infrared (IR) spectroscopy can be used to identify M–H, but their bands can have weak intensity and/or be buried in the IR fingerprint region.[1,12] Furthermore, X-ray-based characterization methods are of limited value because of the low X-ray scattering factors of lighter elements.[13,14] Conversely, neutron-based techniques, such as inelastic neutron scattering (INS) are well suited to the analysis of M–H species and their structural features, though large amounts of sample and access to a spallation source are required.[15–19]

In contrast, nuclear magnetic resonance (NMR) spectroscopy is a particularly powerful tool for identifying metal hydrides that display a broad range of ^{1}H chemical shifts (δ, varying from +35 to −60 ppm) depending on the configuration of the metal sites and its ligands.[20–22] Nonetheless, the interpretation of the ^{1}H chemical shift is challenging as the chemical shift is often dominated by the 'spin-orbit heavy-atom effect on the light-atom' (SO-HALA effect).[20,23–25] In that context, the use of ^{2}H ssNMR is noteworthy since deuterium, as a quadrupolar nucleus ($I=1$), interacts with the electric field gradient (EFG), providing insights into the distribution of charge about the nucleus.[26,27] Thus, the ^{2}H ssNMR signal can provide insights into

Supporting information for this article is available on the WWW under https://doi.org/10.1002/hlca.202300173

the ionicity of a metal hydrogen bond based on the deuteride isotopologue (M–D) because the magnitude of the quadrupolar coupling constant (C_Q) decreases for more polarized M–D bonds.[26,27] Further insights into the binding mode of an M–D bond are obtained by looking at the asymmetry parameter (η), where $\eta = 0$ is characteristic of a terminal M–D, while $\eta > 0.1$ is indicative of bridging M–D.[26–30]

Here, we investigate the ^{2}H ssNMR of supported M–D species, derived from silica-supported zirconium hydrides (Zr(H)@SiO_2, *Figure 1,a*), prepared through Surface Organometallic Chemistry (SOMC).[26,27,29,31] These materials, that are able to convert hydrocarbons and polymers under mild conditions,[6–8,32–35] have been shown to contain two distinct surface species, the mono-hydride (≡SiO)$_3$Zr–H and the bis-hydride (≡SiO)$_2$Zr(H)$_2$. In this work, the NMR signatures of the corresponding deuteride species are measured and compared to molecular zirconocene analogues, which are used to better understand the factors influencing the EFG parameters of M–D bonds in early-transition metal deuterides,[26,27,29,31] and to benchmark Density Functional Theory (DFT) calculations (*Figure 1,b*).

Results and Discussion

The low natural abundance of deuterium (0.012%) necessitates isotopic enrichment of samples to enable acquisition of high quality ^{2}H-NMR spectra.[36] Thus, we first synthesized the deuteride analog of Schwartz's Reagent [(Cp)$_2$ZrCl(μ$_2$-D)]$_2$ (Cp$^-$ = cyclopentadienyl), a widely used reagent in organic synthesis, and the corresponding *bis*-deuteride [(Cp)$_2$ZrD(μ$_2$-D)]$_2$ as benchmark systems (For synthesis, see *Supporting Information S2*).

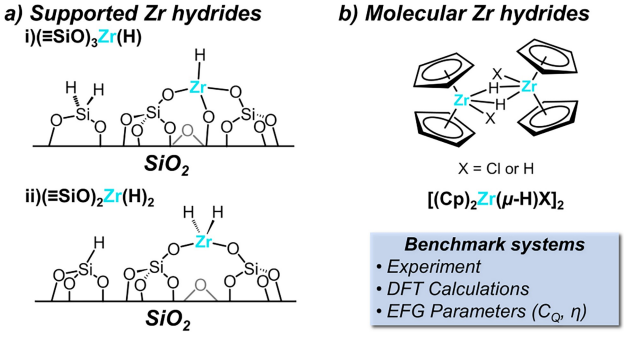

Figure 1. Overview of work. a) Proposed Zr–H species in silica-supported zirconium hydrides (Zr(H)@SiO_2), and b) molecular Zr-hydrides as benchmark.

Despite widespread use, to the best of our knowledge, there is no reported X-ray crystal structure for [(Cp)$_2$ZrCl(μ$_2$-H)]$_2$. However, its dimeric structure has been confirmed by microcrystal electron diffraction (MicroED),[37] and analysis of the ^{35}Cl solid-state NMR signature,[38] paralleling the structure of the corresponding substituted zirconocene equivalents.[39,40] Similarly, for [(Cp)$_2$ZrH(μ$_2$-H)]$_2$, no single-crystal X-ray crystal structure has been reported. However, by analogy with related structures containing substituted Cp rings, this compound likely contains both a terminal hydride ligand on each Zr, and two bridging hydrides (μ$_2$-H).[41–46]

The magic-angle spinning (MAS) ^{2}H-NMR spectrum of [(Cp)$_2$ZrCl(μ$_2$-D)]$_2$, measured at 14.1 T and 107 K, gives a spinning sideband manifold consistent with a single species with isotropic chemical shift (δ_{iso}) of 0 ppm (*Figure 2,a*). Fitting of this signal gives a C_Q and η equal to 50 kHz and 0.38, respectively. The C_Q value matches the previously reported values for Zr–D motifs,[30,31] while the value of η is consistent with the values expected for a bridging μ$_2$-D species.[26,27,47] Analysis of the ^{2}H MAS spectrum of [(Cp)$_2$ZrD(μ^2-D)]$_2$ (*Figure 2,b*), gives two spinning sideband manifolds with δ_{iso} of +3.8 and −3.5 ppm, consistent with the reported chemical shifts in solution.[48] Fitting of the signal at 3.8 ppm gives a C_Q and η of 47 kHz and 0.00, respectively. Again, the C_Q is close to previously reported values for Zr–D motifs,[30,31] while η is consistent with that of a terminal deuteride.[26–29,47] By contrast, the signal at −3.5 ppm is associated with $C_Q = 46$ kHz and $\eta = 0.37$, consistent with a μ$_2$-D species (*vide supra*).[41–46] In both cases, the magnitude of the C_Q indicates the presence of a relatively ionic M–D bond (*i.e.* M$^{\delta+}$-D$^{\delta-}$), with a C_Q lower than that of more covalent M–D bonds of late transition metals (typically > 50 kHz).[27–29,49]

To confront the experimental EFG parameters, we turned to calculations of NMR parameters using DFT (*Supporting Information S4*). The calculated NMR parameters of [(Cp)$_2$ZrCl(μ$_2$-D)]$_2$ with two equivalent μ$_2$-D ($C_Q = 48.9$ kHz and $\eta = 0.31$) match experimental values ($C_Q = 50$ kHz and $\eta = 0.38$). Notably, the calculated values for a monomeric zirconocene deuteride chloride structure ($C_Q = 44.0$ kHz, $\eta = 0.12$), akin to that reported for Cp$^-$ derivatives with bulky substituents,[50] are not consistent with the experimental line shape, further supporting the dimeric structure and illustrating the dependence of η on the mode of M–D bonding (*Supporting Information S4*). For [(Cp)$_2$ZrD(μ$_2$-D)]$_2$, calculated C_Q values for the terminal (D) and bridging (μ$_2$-D) hydrides (*Figure 3*) are 44.2 and

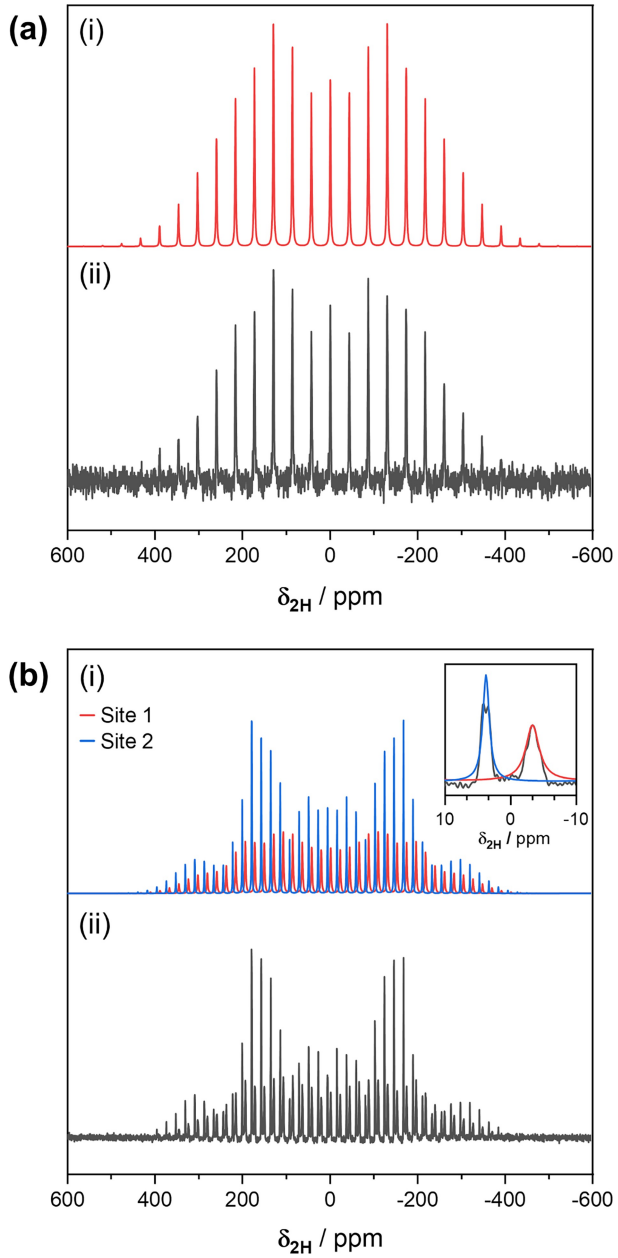

Figure 2. ^{2}H-NMR of molecular zirconium deuterides. (a) $[(Cp)_2ZrCl(\mu_2\text{-}D)]_2$ (i) fit of experimental data, (ii) experimental data (14.1 T, MAS 4 kHz, 107 K). (b) $[(Cp)_2ZrD(\mu_2\text{-}D)]_2$ (i) fit of experimental data (Site 1, red; site 2, blue) (ii) experimental data (14.1 T, MAS 2 kHz, 107 K), inset shows isotropic region.

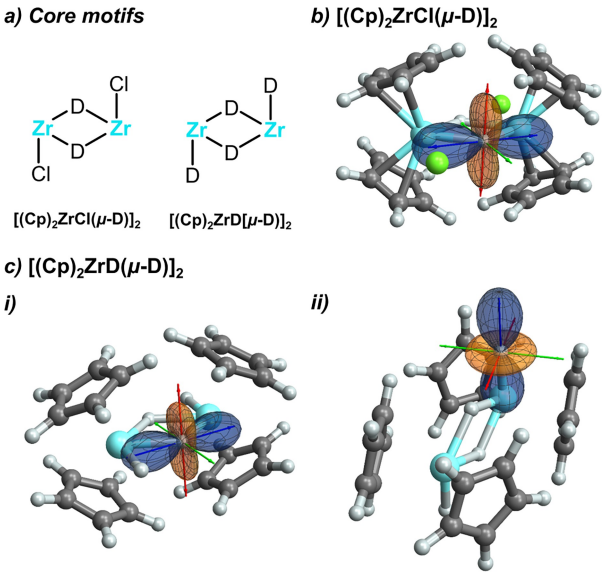

Figure 3. Visualization of EFG tensors for M–D species in zirconocene hydrides. a) Top-view of core motifs for dimeric zirconocene hydrides. b) Projection of EFG tensor for bridging deuteride in $[(Cp)_2ZrCl(\mu_2\text{-}D)]_2$; c) i) EFG tensor for bridging deuteride in $[(Cp)_2ZrD(\mu_2\text{-}D)]_2$, ii) EFG tensor for terminal deuteride in $[(Cp)_2ZrD(\mu_2\text{-}D)]_2$. Orientation of V_{ZZ} represented by blue axis, V_{YY} by red, and V_{XX} by green.

41.7 kHz, respectively. These values offer good agreement with the experimentally determined C_Q for terminal and bridged hydrides (47 and 46 kHz, resp.). The values of η for the terminal and bridged species also reflect those obtained from experiment (0.00 (calc.) *vs.* 0.00 (expt.) and 0.30 (calc.) *vs.* 0.37 (expt.), resp.), showing that while terminal and bridging Zr–D have similar C_Q, they are easily distinguished by η.[26]

The calculated EFG tensors for $[(Cp)_2ZrCl(\mu_2\text{-}D)]_2$ are visualized in *Figure 3,b*. From the EFG tensor of the dimeric structure the largest component ($|V_{ZZ}|$) lies on the M–D–M plane parallel to the Zr–Zr axis. The second largest component of the calculated tensor ($|V_{YY}|$) lies perpendicular to the M–D–M plane, and is appreciably larger than the 3rd component ($|V_{XX}|$) – accounting for the observed non-zero value of η. For $[(Cp)_2ZrD(\mu_2\text{-}D)]_2$, the orientation of the EFG tensor for the bridged deuteride is similar to that of $[(Cp)_2ZrCl(\mu_2\text{-}D)]_2$ (*Figure 3,c*). By contrast, for the terminal deuteride, V_{ZZ} lies along the M–D bond, and the tensor is axially symmetric about the M–D bond (*i.e.* $V_{YY} \approx V_{XX}$), as previously reported.[27] In sum, calculations and experiment offer good agreement for these benchmark systems, illustrating that C_Q and η provide insights into the ionicity of M–D bonds and enable distinction of terminal/bridged M–D species, respectively.

Thus, the approach was extended to surface hydride species, focusing on well-defined zirconium deuterides. Zirconium hydride species ($Zr(H)@SiO_2$) were generated by grafting $Zr(CH_2{}^tBu)_4$ on a silica partially dehydroxylated at 500 °C (SiO_{2-500}) followed by a treatment under H_2, as previously described (*Supporting Information S3*).[6–8,32–35] Analysis of Zr(H)-

@SiO_2 by infrared (IR) spectroscopy reveals bands assigned to Si–H and Zr–H.[51–53] The two bands at 2262 and 2194 cm^{-1} are attributed to Si–H species, while three distinct Zr–H bands are observed and are attributed to Zr(H) (1638 cm^{-1}) and $Zr(H)_2$ (1650 and 1623 cm^{-1}), based on earlier literature (*Supporting Information S3*).[52] The ^{1}H-NMR of Zr(H)@SiO_{2-500} shows peaks at 12 ppm, 10 ppm, 4.3 ppm and 0.7 ppm (*Supporting Information S3*), that correspond to Zr-(H)$_2$, Zr–*H*, Si–*H* and C–*H*, respectively, based on previous studies.[53,54]

Subsequently, H/D exchange was performed using D_2 on Zr(H)@SiO_2, to introduce the deuterium to the exchangeable sites on the surface (full experimental details in the *Supporting Information S3*). Analysis of the H/D exchanged material (henceforth referred to as Zr(H/D)@SiO_2), using IR spectroscopy suggests that both Si–H and Zr–H species are partially exchanged during the reaction, as illustrated by the partial depletion of bands between 2260–2200 cm^{-1} and 1650–1620 cm^{-1}, respectively. The partial exchange of Zr–H is also evidenced by ^{1}H-NMR, with remaining resonance at 12 and 10 ppm.[53] Notably, while the bands at 1650 and 1623 cm^{-1} in the IR spectrum, previously assigned to $Zr(H)_2$, are depleted more rapidly than the central band at 1638 cm^{-1}, attributed to Zr(H) (*Supporting Information S3*),[52] the inverse is observed in ^{1}H-NMR where a more extensive depletion of the peak at 10 ppm (Zr(H)) vs. 12 ppm ($Zr(H)_2$), is observed (*Supporting Information S3*).[53,54] This apparent discrepancy likely shows that the attribution of IR bands is more complex than previously proposed.

Analysis of Zr(H/D)@SiO_{2-500} by means of ^{2}H-NMR at low temperature (*ca.* 110 K) reveals the presence of multiple resonances (*Figure 4,a* and *4,b*, *Supporting Information S3*). The dominant peaks (at 5.2 and 4.3 ppm) are assigned to Si–D, formed through exchange with Si–H, as indicated previously by analysis of IR, the observed C_Q ($C_{Q(Obs)}$) values for these species (58 and 42 kHz) are lower than calculated values from fluoride-terminated SiO_2 cluster models (88–94 kHz, see *Supporting Information* S4), or reported values for Si–D in molecular systems (90–95 kHz),[55–57] suggesting residual dynamics for these species that decrease the observed C_Q.[58–60] Two smaller peaks are also present – a peak at 1.5 ppm, which is assigned to C–D resonances of the remaining alkyl groups, which again has a reduced $C_{Q(Obs)}$ (96 kHz) relative to typical values for a C–D bond (likely as a result of residual dynamics).[58–61] In addition, a peak centered at 9.8 ppm, which is assigned to Zr–D species, is observed. Fitting of the

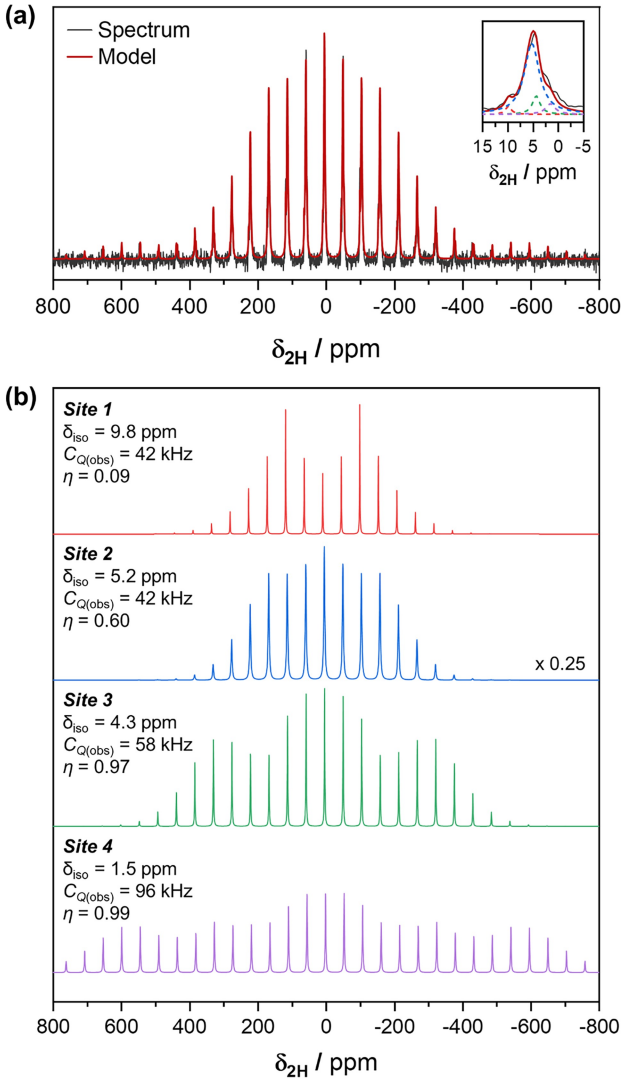

Figure 4. (a) ^{2}H ssNMR of Zr(H/D)@SiO_2 (14.1 T, 111 K, MAS:5 kHz). (b) Decomposition of fit for Zr(H/D)@SiO_2, site 2 rescaled for clarity. (c) Visualization of EFG tensors for fluoride-terminated SiO_2 cluster models of i) (≡SiO)$_3$Zr(D)) and ii) (≡SiO)$_2$Zr(D)$_2$. Orientation of V_{ZZ} represented by blue axis, V_{YY} by red, and V_{XX} by green.

site at 9.8 ppm gives a value of η of 0.09 and C_Q of 42 kHz (*Figure 4,b*), consistent with terminal Zr–D (*vide infra*).[53] We note that low temperatures (< 200 K) are required to observe the full spinning sideband manifold for M–D surface species in Zr(H)@SiO_2, while the $C_{Q(obs)}$ for Si–D and C–D bonds in the same material are lower than expected for the respective bonds. This is likely due to residual dynamics that average quadrupolar interactions.

Notably, under the conditions employed it was not possible to observe multiple distinct resonances in the range 12–10 ppm (*i.e.*, the range expected for Zr–D). However, based on the ^{1}H-NMR it is likely that the site at 12 ppm is not reacting readily with the D_2 gas under the conditions explored. The incomplete exchange of Zr–H upon exposure to D_2 is consistent with earlier studies on silica-supported metal hydrides, suggesting a distribution of Zr–H sites, whose reactivities depends on the local coordination environment, *e.g.*, presence of additional interaction with adjacent siloxane bridges.[62,63]

Calculations of NMR parameters (δ_{iso} and EFG tensors) of the proposed surface deuteride species, for both $(\equiv SiO)_3Zr(D)$ and $(\equiv SiO)_2Zr(D)_2$, were also evaluated, using models based on fluoride-terminated SiO_2 clusters (*Figure 4,c*). Consistent with earlier studies by ^{1}H ssNMR, the chemical shift of $(\equiv SiO)_3Zr(D)$) and $(\equiv SiO)_2Zr(D)_2$, were calculated to be 10.8 and 11.6 ppm, respectively.[53,54] In both cases, the C_Q of the corresponding deuteride was found to be *ca.* 40 kHz (*Supporting Information S4*), indicating a relatively ionic Zr–D bond as in the zirconocene homologues. As expected for a terminal hydride, η is close to zero (0.00 and 0.01) in both cases. Visualization of the calculated EFG tensors for the $(\equiv SiO)_3Zr(D)$ and $(\equiv SiO)_2Zr(D)_2$ models are shown in *Figure 4,c*. In both cases, V_{ZZ} is oriented along the M–D bond, as observed for the molecular zirconocene models. Both calculated and experimental structures are consistent with the presence of terminal M–D.

Conclusions

To conclude, ^{2}H ssNMR is shown to be a powerful tool to probe the structure of supported M-D/H species, here focusing on the prototypical silica-supported zirconium hydrides prepared through SOMC. The Zr-deuteride species detected at the surface of Zr(H/D)@SiO_{2-700} correspond to terminal M–D as indicated by the low value of η ($\eta \approx 0$), while the magnitude of the C_Q (*ca.* 40 kHz) highlights the rather ionic Zr–D bonds, as observed in the zirconocene homologues – contrasting what is known for late transition metal hydrides. We are currently extending this approach to study a broad range of molecular and oxide-supported metal hydrides.

Experimental Section

Synthesis of Molecular Compounds

$[(Cp)_2Zr(H)Cl]_2$ and $[(Cp)_2ZrH_2]_2$ were synthesized using an adapted literature procedure.[64] The corresponding deuterides were synthesized analogously, using $LiAlD_4$ in place of $LiAlH_4$. Tetrakis(2,2-dimethylpropyl)-zirconium ($ZrNp_4$) was synthesized using an adapted literature procedure.[35] Further details for the synthesis and characterization of the molecules used are provided in the *Supporting Information*.

Synthesis of Supported Zr Species

$ZrNp_x@SiO_2$, Zr(H)@SiO_{2-500} and Zr(H/D)@SiO_{2-500} were synthesized using an adapted literature procedure starting from silica partially dehydroxylated at 500 °C (SiO_{2-500}) and $ZrNp_4$.[53] Further details for the synthesis and characterization of the molecules used are provided in the *Supporting Information*.

Computational Details

Geometry optimization was performed using a hybrid PBE0/TZ2P level of theory including the extra basis set Stuttgart/Dresden ECPs (SDD) for Zr atoms using Gaussian09.[65–68] NMR and EFG calculations were performed for geometry optimized structures using a hybrid PBE0/TZ2P[65,69–71] level of theory that included contributions from spin-orbit coupling using the zeroth-order regular approximation (ZORA)[72–75] by ADF2022.[76]

Supporting Information

The authors have cited additional references within the *Supporting Information*.[77–86]

Author Contribution Statement

S. R. D and C. C. conceived the project. S. R. D. and P. S. synthesized all molecules and materials and performed all routine characterization. Solid-state ^{2}H-NMR experi-

ments were performed and analyzed by S. R. D., P. S. and A. V. Y. Calculations at the DFT-level were performed by P. S., D. G. and A. V. Y. All authors participated in formal analysis, writing and editing of the work.

Acknowledgements

C. C. and S. R. D. acknowledge the Swiss National Science Foundation (grants 200021_169134, and 200020B_192050). C. C. and A. V. Y. gratefully acknowledge ETH + Project SynthMatLab for the financial support. D. G. and C. C. gratefully acknowledge the Swiss National Science Foundation (grants 200020B_192050 and 200021 L_213070).

Data Availability Statement

The data that support the findings of this study are available from the corresponding author upon reasonable request.

References

[1] C. Copéret, D. P. Estes, K. Larmier, K. Searles, 'Isolated Surface Hydrides: Formation, Structure, and Reactivity', *Chem. Rev.* **2016**, *116*, 8463–8505.
[2] Z. Maeno, S. Yasumura, X. Wu, M. Huang, C. Liu, T. Toyao, K. Shimizu, 'Isolated Indium Hydrides in CHA Zeolites: Speciation and Catalysis for Nonoxidative Dehydrogenation of Ethane', *J. Am. Chem. Soc.* **2020**, *142*, 4820–4832.
[3] V. Vidal, A. Théolier, J. Thivolle-Cazat, J.-M. Basset, 'Metathesis of Alkanes Catalyzed by Silica-Supported Transition Metal Hydrides', *Science* **1997**, *276*, 99–102.
[4] E. S. Wiedner, M. B. Chambers, C. L. Pitman, R. M. Bullock, A. J. M. Miller, A. M. Appel, 'Thermodynamic Hydricity of Transition Metal Hydrides', *Chem. Rev.* **2016**, *116*, 8655–8692.
[5] G. L. Casty, M. G. Matturro, G. R. Myers, R. P. Reynolds, R. B. Hall, 'Hydrogen/Deuterium Exchange Kinetics by a Silica-Supported Zirconium Hydride Catalyst: Evidence for a σ-Bond Metathesis Mechanism', *Organometallics* **2001**, *20*, 2246–2249.
[6] Y. I. Yermakov, B. N. Kuznetsov, 'Supported metallic catalysts prepared by decomposition of surface ornagometallic complexes', *J. Mol. Catal.* **1980**, *9*, 13–40.
[7] Y. I. Yermakov, Y. A. Ryndin, O. S. Alekseev, D. I. Kochubey, V. A. Shmachkov, N. I. Gergert, 'Hydride complexes of titanium and zirconium attached to SiO_2 as hydrogenation catalysts', *J. Mol. Catal.* **1989**, *49*, 121–132.
[8] J. Corker, F. Lefebvre, C. Lécuyer, V. Dufaud, F. Quignard, A. Choplin, J. Evans, J.-M. Basset, 'Catalytic Cleavage of the C–H and C–C Bonds of Alkanes by Surface Organometallic Chemistry: An EXAFS and IR Characterization of a Zr–H Catalyst', *Science* **1996**, *271*, 966–969.
[9] J.-M. Basset, C. Coperet, D. Soulivong, M. Taoufik, J. T. Cazat, 'Metathesis of Alkanes and Related Reactions', *Acc. Chem. Res.* **2010**, *43*, 323–334.
[10] U. Kanbur, G. Zang, A. L. Paterson, P. Chatterjee, R. A. Hackler, M. Delferro, I. I. Slowing, F. A. Perras, P. Sun, A. D. Sadow, 'Catalytic carbon-carbon bond cleavage and carbon-element bond formation give new life for polyolefins as biodegradable surfactants', *Chem* **2021**, *7*, 1347–1362.
[11] V. Dufaud, J.-M. Basset, 'Catalytic Hydrogenolysis at Low Temperature and Pressure of Polyethylene and Polypropylene to Diesels or Lower Alkanes by a Zirconium Hydride Supported on Silica-Alumina: A Step Toward Polyolefin Degradation by the Microscopic Reverse of Ziegler–Natta Pol', *Angew. Chem. Int. Ed.* **1998**, *37*, 806–810.
[12] A. J. Jordan, G. Lalic, J. P. Sadighi, 'Coinage Metal Hydrides: Synthesis, Characterization, and Reactivity', *Chem. Rev.* **2016**, *116*, 8318–8372.
[13] M. Woińska, S. Grabowsky, P. M. Dominiak, K. Woźniak, D. Jayatilaka, 'Hydrogen atoms can be located accurately and precisely by x-ray crystallography', *Sci. Adv.* **2023**, *2*, e1600192.
[14] M. Schmidtmann, P. Coster, P. F. Henry, V. P. Ting, M. T. Weller, C. C. Wilson, 'Determining hydrogen positions in crystal engineered organic molecular complexes by joint neutron powder and single crystal X-ray diffraction', *CrystEngComm* **2014**, *16*, 1232–1236.
[15] F. Polo-Garzon, S. Luo, Y. Cheng, K. L. Page, A. J. Ramirez-Cuesta, P. F. Britt, Z. Wu, 'Neutron Scattering Investigations of Hydride Species in Heterogeneous Catalysis', *ChemSusChem* **2019**, *12*, 93–103.
[16] S. F. Parker, S. Mukhopadhyay, M. Jiménez-Ruiz, P. W. Albers, 'Adsorbed States of Hydrogen on Platinum: A New Perspective', *Chem. Eur. J.* **2019**, *25*, 6496–6499.
[17] E. L. Bennett, P. J. Murphy, S. Imberti, S. F. Parker, 'Characterization of the Hydrides in Stryker's Reagent: $[HCu\{P(C_6H_5)_3\}]_6$', *Inorg. Chem.* **2014**, *53*, 2963–2967.
[18] T. J. Hebden, K. I. Goldberg, D. M. Heinekey, X. Zhang, T. J. Emge, A. S. Goldman, K. Krogh-Jespersen, 'Dihydrogen/Dihydride or Tetrahydride? An Experimental and Computational Investigation of Pincer Iridium Polyhydrides', *Inorg. Chem.* **2010**, *49*, 1733–1742.
[19] V. J. Murphy, D. Rabinovich, T. Hascall, W. T. Klooster, T. F. Koetzle, G. Parkin, 'False Minima in X-ray Structure Solutions Associated with a "Partial Polar Ambiguity": Single Crystal X-ray and Neutron Diffraction Studies on the Eight-Coordinate Tungsten Hydride Complexes, $W(PMe_3)_4H_2X_2$ (X=F, Cl, Br, I) and $W(PMe_3)_4H_2F(FHF)$', *J. Am. Chem. Soc.* **1998**, *120*, 4372–4387.
[20] J. Vícha, J. Novotný, S. Komorovsky, M. Straka, M. Kaupp, R. Marek, 'Relativistic Heavy-Neighbor-Atom Effects on NMR Shifts: Concepts and Trends Across the Periodic Table', *Chem. Rev.* **2020**, *120*, 7065–7103.
[21] S. Bhagan, B. B. Wayland, 'Formation and Reactivity of a Porphyrin Iridium Hydride in Water: Acid Dissociation Constants and Equilibrium Thermodynamics Relevant to Ir–H, Ir–OH, and Ir–CH_2– Bond Dissociation Energetics', *Inorg. Chem.* **2011**, *50*, 11011–11020.
[22] J. Schneider, C. P. Sindlinger, K. Eichele, H. Schubert, L. Wesemann, 'Low-Valent Lead Hydride and Its Extreme

Low-Field ^{1}H-NMR Chemical Shift', *J. Am. Chem. Soc.* **2017**, *139*, 6542–6545.
[23] J. Vícha, S. Komorovsky, M. Repisky, R. Marek, M. Straka, 'Relativistic Spin–Orbit Heavy Atom on the Light Atom NMR Chemical Shifts: General Trends Across the Periodic Table Explained', *J. Chem. Theory Comput.* **2018**, *14*, 3025–3039.
[24] P. Pyykkö, A. Görling, N. Rösch, 'A transparent interpretation of the relativistic contribution to the N. M. R. 'heavy atom chemical shift'', *Mol. Phys.* **1987**, *61*, 195–205.
[25] U. Edlund, T. Lejon, P. Pyykkö, T. K. Venkatachalam, E. Buncel, 'Lithium-7, silicon-29, tin-119, and lead-207 NMR studies of phenyl-substituted Group 4 anions', *J. Am. Chem. Soc.* **1987**, *109*, 5982–5985.
[26] A. J. Kim, F. R. Fronczek, L. G. Butler, S. Chen, E. A. Keiter, 'Deuterium quadrupole coupling constants and asymmetry parameters in bridging metal hydride complexes', *J. Am. Chem. Soc.* **1991**, *113*, 9090–9096.
[27] L. G. Butler, E. A. Keiter, 'Interpretation of electric field gradients at deuterium as measured by solid-state NMR spectroscopy', *J. Coord. Chem.* **1994**, *32*, 121–134.
[28] B. Walaszek, A. Adamczyk, T. Pery, X. Yeping, T. Gutmann, N. de S. Amadeu, S. Ulrich, H. Breitzke, H. M. Vieth, S. Sabo-Etienne, B. Chaudret, H.-H. Limbach, G. Buntkowsky, '^{2}H Solid-State NMR of Ruthenium Complexes', *J. Am. Chem. Soc.* **2008**, *130*, 17502–17508.
[29] T. Gutmann, B. Walaszek, X. Yeping, M. Wächtler, I. del Rosal, A. Grünberg, R. Poteau, R. Axet, G. Lavigne, B. Chaudret, H.-H. Limbach, G. Buntkowsky, 'Hydrido-Ruthenium Cluster Complexes as Models for Reactive Surface Hydrogen Species of Ruthenium Nanoparticles. Solid-State ^{2}H-NMR and Quantum Chemical Calculations', *J. Am. Chem. Soc.* **2010**, *132*, 11759–11767.
[30] D. B. Culver, R. W. Dorn, A. Venkatesh, J. Meeprasert, A. J. Rossini, E. A. Pidko, A. S. Lipton, G. R. Lief, M. P. Conley, 'Active Sites in a Heterogeneous Organometallic Catalyst for the Polymerization of Ethylene', *ACS Cent. Sci.* **2021**, *7*, 1225–1231.
[31] W. L. Jarrett, R. D. Farlee, L. G. Butler, 'Observation of bridging and terminal metal hydrides by solid-state deuterium NMR spectroscopy: application to bis-(cyclopentadienyl)zirconium dideuteride', *Inorg. Chem.* **1987**, *26*, 1381–1383.
[32] V. A. Zakharov, V. K. Dudchenko, E. A. Paukshtis, L. G. Karakchiev, Y. I. Yermakov, 'Formation of zirconium hydrides in supported organozirconium catalysts and their role in ethylene polymerization', *J. Mol. Catal.* **1977**, *2*, 421–435.
[33] J. Schwartz, M. D. Ward, 'Silica-supported zirconium hydrides as isomerization or hydrogenation catalysts for long-chain olefins', *J. Mol. Catal.* **1980**, *8*, 465–469.
[34] C. Lecuyer, F. Quignard, A. Choplin, D. Olivier, J.-M. Basset, 'Surface Organometallic Chemistry on Oxides: Selective Catalytic Low-Temperature Hydrogenolysis of Alkanes by a Highly Electrophilic Zirconium Hydride Complex Supported on Silica', *Angew. Chem. Int. Ed.* **1991**, *30*, 1660–1661.
[35] S. A. King, J. Schwartz, 'Chemistry of (silica)zirconium dihydride', *Inorg. Chem.* **1991**, *30*, 3771–3774.
[36] K. J. R. Rosman, P. D. P. Taylor, 'Isotopic compositions of the elements 1997 (Technical Report)', *Pure Appl. Chem.* **1998**, *70*, 217–235.
[37] C. G. Jones, M. Asay, L. J. Kim, J. F. Kleinsasser, A. Saha, T. J. Fulton, K. R. Berkley, D. Cascio, A. G. Malyutin, M. P. Conley, B. M. Stoltz, V. Lavallo, J. A. Rodríguez, H. M. Nelson, 'Characterization of Reactive Organometallic Species via MicroED', *ACS Cent. Sci.* **2019**, *5*, 1507–1513.
[38] A. J. Rossini, R. W. Mills, G. A. Briscoe, E. L. Norton, S. J. Geier, I. Hung, S. Zheng, J. Autschbach, R. W. Schurko, 'Solid-State Chlorine NMR of Group IV Transition Metal Organometallic Complexes', *J. Am. Chem. Soc.* **2009**, *131*, 3317–3330.
[39] K. P. Reddy, J. L. Petersen, 'Synthesis and characterization of binuclear zirconocenophane hydrides. The molecular structure of $[SiMe_2(C_5H_4)_2][(\eta^5\text{-}C_5H_5)ZrCl(\mu\text{-}H)]_2$', *Organometallics* **1989**, *8*, 547–549.
[40] M. Bochmann, S. J. Lancaster, M. B. Hursthouse, M. Mazid, 'Synthesis and Structure of $[Me_2C(C_5H_4)(Flu)Zr(\mu\text{-}H)Cl]_2$, an η^3:η^5-bonded *ansa*-Metallocene', *Organometallics* **1993**, *12*, 4718–4720.
[41] R. Choukroun, F. Dahan, A. M. Larsonneur, E. Samuel, J. Petersen, P. Meunier, C. Sornay, 'Synthesis, X-ray Structure and Electrochemical Study of $[\{\eta^5\text{-}C_5H_4C(CH_3)_3\}_2ZrH(\mu\text{-}H)]_2$. Identification of the $[\{\eta^5\text{-}C_5H_4C(CH_3)_3\}]_2ZrH_2$ Anion Radical by EPR Spectroscopy', *Organometallics* **1991**, *10*, 374–376.
[42] A. M. Larsonneur, R. Choukroun, J. Jaud, 'Synthesis, Characterization, and Chemical Reactivity of Zirconium Dihydride $[(C_5H_4R)_2Zr(\mu\text{-}H)H]_2$ (R=SiMe$_3$, CMe$_3$). H/D Exchange Reactions of Anionic Species $[(C_5H_4R)_2ZrH_2]^-$. X-ray Crystal Structure of $[(C_5H_4SiMe_3)_2Zr(\mu\text{-}H)H]_2$', *Organometallics* **1993**, *12*, 3216–3224.
[43] P. Arndt, A. Spannenberg, W. Baumann, V. V. Burlakov, U. Rosenthal, S. Becke, T. Weiss, 'Reactions of Zirconocene 2-Vinylpyridine Complexes with Diisobutylaluminum Hydride and Fluoride', *Organometallics* **2004**, *23*, 4792–4795.
[44] P. J. Chirik, L. M. Henling, J. E. Bercaw, 'Synthesis of Singly and Doubly Bridged *ansa*-Zirconocene Hydrides. Formation of an Unusual Mixed Valence Trimeric Hydride by Reaction of H_2 with $\{(Me_2Si)_2(\eta^5\text{-}C_5H_3)_2\}Zr(CH_3)_2$ and Generation of a Dinitrogen Complex by Reaction of N_2 with a Zirconocene Dihydride', *Organometallics* **2001**, *20*, 534–544.
[45] G. Bai, P. Müller, H. W. Roesky, I. Usón, 'Intramolecular Coupling of Two Cyclopentadienyl Ring Systems of Zirconium – Unprecedented Formation of a Dihydride and Preparation of the $[\{(MeC_5H_4)Zr\}_5(\mu_5\text{-}N)(\mu_3\text{-}NH)_4(\mu\text{-}NH_2)_4]$ Cluster in a Two-Phase System', *Organometallics* **2000**, *19*, 4675–4677.
[46] S. B. Jones, J. L. Petersen, 'Preparation and Structural Characterization of Early-Transition-Metal Hydrides. $[(\eta^5\text{-}C_5H_4CH_3)_2ZrH(\mu\text{-}H)]_2$, a Binuclear Zirconium Hydride Complex', *Inorg. Chem.* **1981**, *20*, 2889–2894.
[47] I. del Rosal, T. Gutmann, B. Walaszek, I. C. Gerber, B. Chaudret, H.-H. Limbach, G. Buntkowsky, R. Poteau, '^{2}H-NMR calculations on polynuclear transition metal complexes: on the influence of local symmetry and other factors', *Phys. Chem. Chem. Phys.* **2011**, *13*, 20199–20207.
[48] D. G. Bickley, N. Hao, P. Bougeard, B. G. Sayer, R. C. Burns, M. J. McGlinchey, 'Reaction of $[\eta^5\text{-}C_5H_5)_2ZrH(\mu\text{-}H)]_2$ with diphenylacetylene: mechanistic and theoretical considerations', *J. Organomet. Chem.* **1983**, *246*, 257–268.
[49] D. Nietlispach, V. I. Bakhmutov, H. Berke, 'Deuterium Quadrupole Coupling Constants and Ionic Bond Character in Transition Metal Hydride Complexes from ^{2}H-NMR T_1

Relaxation Data in Solution', *J. Am. Chem. Soc.* **1993**, *115*, 9191–9195.
[50] J. A. Pool, C. A. Bradley, P. J. Chirik, 'A Convenient Method for the Synthesis of Zirconocene Hydrido Chloride, Isobutyl Hydride, and Dihydride Complexes Using *tert*-Butyl Lithium', *Organometallics* **2002**, *21*, 1271–1277.
[51] F. Quignard, C. Lécuyer, A. Choplin, D. Olivier, J.-M. Basset, 'Surface organometallic chemistry of zirconium: Application to the stoichiometric activation of the C–H bonds of alkanes and to the low-temperature catalytic hydrogenolysis of alkanes', *J. Mol. Catal.* **1992**, *74*, 353–363.
[52] C. Thieuleux, E. A. Quadrelli, J.-M. Basset, J. Döbler, J. Sauer, 'Methane activation by silica-supported Zr(IV) hydrides: the dihydride $[(\equiv SiO)_2ZrH_2]$ is much faster than the monohydride $[(\equiv SiO)_3ZrH]$', *Chem. Commun.* **2004**, 1729–1731.
[53] F. Rataboul, A. Baudouin, C. Thieuleux, L. Veyre, C. Copéret, J. Thivolle-Cazat, J.-M. Basset, A. Lesage, L. Emsley, 'Molecular Understanding of the Formation of Surface Zirconium Hydrides upon Thermal Treatment under Hydrogen of $[(\equiv SiO)Zr(CH_2tBu)_3]$ by Using Advanced Solid-State NMR Techniques', *J. Am. Chem. Soc.* **2004**, *126*, 12541–12550.
[54] M. P. Kalhor, R. Wischert, C. Copéret, H. Chermette, 'Reactivity of silica supported zirconium hydride towards N_2O and CO_2 probe molecules: a computational point of view', *New J. Chem.* **2014**, *38*, 3717–3721.
[55] U. Lähteenmäki, L. Niemelä, P. Pyykkö, 'Deuteron magnetic resonance in solid and liquid SiD_4 above 36°K', *Phys. Lett. A* **1967**, *25*, 460–461.
[56] R. Ader, A. Loewenstein, 'N. M. R. study of methylsilane-d_3 dissolved in a nematic liquid crystal', *Mol. Phys.* **1974**, *27*, 1113–1116.
[57] B.-M. Fung, I. Y. Wei, 'Proton and Deuteron Magnetic Resonance of Phenylsilane-d_3, Phenylphosphine-d_2, and Benzenethiol-*d* in Liquid Crystal Solutions', *J. Am. Chem. Soc.* **1970**, *92*, 1497–1501.
[58] M. Fechtelkord, 'Influence of Sodium Ion Dynamics on the ^{23}Na Quadrupolar Interaction in Sodalite: A High-Temperature ^{23}Na MAS NMR Study', *Solid State Nucl. Magn. Reson.* **2000**, *18*, 70–88.
[59] G. H. Penner, J. M. Polson, S. I. Daleman, K. Reid, 'A deuterium NMR study of molecular dynamics and geometry in two classes of onium salts: $(CH_3)_3E^+X^-$ and $C_6H_5M(CH_3)_3{}^+I^-$', *Can. J. Chem.* **1993**, *71*, 417–426.
[60] E. G. Keeler, V. K. Michaelis, R. G. Griffin, '^{17}O NMR Investigation of Water Structure and Dynamics', *J. Phys. Chem. B* **2016**, *120*, 7851–7858.
[61] L. Vugmeyster, D. Ostrovsky, 'Basic experiments in ^{2}H static NMR for the characterization of protein side-chain dynamics', *Methods* **2018**, *148*, 136–145.
[62] S. Soignier, M. Taoufik, E. Le Roux, G. Saggio, C. Dablemont, A. Baudouin, F. Lefebvre, A. de Mallmann, J. Thivolle-Cazat, J.-M. Basset, G. Sunley, B. M. Maunders, 'Tantalum Hydrides Supported on MCM-41 Mesoporous Silica: Activation of Methane and Thermal Evolution of the Tantalum-Methyl Species', *Organometallics* **2006**, *25*, 1569–1577.
[63] G. Tosin, C. C. Santini, A. Baudouin, A. De Mallman, S. Fiddy, C. Dablemont, J.-M. Basset, 'Reactivity of Silica-Supported Hafnium Tris-neopentyl with Dihydrogen: Formation and Characterization of Silica Surface Hafnium Hydrides and Alkyl Hydride', *Organometallics* **2007**, *26*, 4118–4127.
[64] S. L. Buchwald, S. J. LaMaire, R. B. Nielsen, B. T. Watson, S. M. King, 'A Modified Procedure for the Preparation of $Cp_2Zr(H)Cl$ (Schwartz's Reagent)', *Tetrahedron Lett.* **1987**, *28*, 3895–3898.
[65] C. Adamo, V. Barone, 'Toward reliable density functional methods without adjustable parameters: The PBE0 model', *J. Chem. Phys.* **1999**, *110*, 6158–6170.
[66] 'Gaussian 09.A', M. J. Frisch, G. W. Trucks, H. B. Schlegel, G. E. Scuseria, M. A. Robb, J. R. Cheeseman, G. Scalmani, V. Barone, G. A. Petersson, H. Nakatsuji, X. Li, M. Caricato, A. Marenich, J. Bloino, B. G. Janesko, R. Gomperts, B. Mennucci, H. P. Hratchian, J. V. Ortiz, A. F. Izmaylov, J. L. Sonnenberg, D. Williams-Young, F. Ding, F. Lipparini, F. Egidi, J. Goings, B. Peng, A. Petrone, T. Henderson, D. Ranasinghe, V. G. Zakrzewski, J. Gao, N. Rega, G. Zheng, W. Liang, M. Hada, M. Ehara, K. Toyota, R. Fukuda, J. Hasegawa, M. Ishida, T. Nakajima, Y. Honda, O. Kitao, H. Nakai, T. Vreven, K. Throssell, J. A. Montgomery Jr., J. E. Peralta, F. Ogliaro, M. Bearpark, J. J. Heyd, E. Brothers, K. N. Kudin, V. N. Staroverov, T. Keith, R. Kobayashi, J. Normand, K. Raghavachari, A. Rendell, J. C. Burant, S. S. Iyengar, J. Tomasi, M. Cossi, J. M. Millam, M. Klene, C. Adamo, R. Cammi, J. W. Ochterski, R. L. Martin, K. Morokuma, O. Farkas, J. B. Foresman, D. J. Fox, Gaussian, Inc., Wallingford CT, 2016.
[67] F. Weigend, R. Ahlrichs, 'Balanced basis sets of split valence, triple zeta valence and quadruple zeta valence quality for H to Rn: Design and assessment of accuracy', *Phys. Chem. Chem. Phys.* **2005**, *7*, 3297–3305.
[68] P. Fuentealba, H. Preuss, H. Stoll, L. Von Szentpály, 'A proper account of core-polarization with pseudopotentials: single valence-electron alkali compounds', *Chem. Phys. Lett.* **1982**, *89*, 418–422.
[69] E. Van Lenthe, E. J. Baerends, 'Optimized Slater-type basis sets for the elements 1–118', *J. Comput. Chem.* **2003**, *24*, 1142–1156.
[70] D. P. Chong, E. Van Lenthe, S. Van Gisbergen, E. J. Baerends, 'Even-tempered slater-type orbitals revisited: From hydrogen to krypton', *J. Comput. Chem.* **2004**, *25*, 1030–1036.
[71] D. P. Chong, 'Augmenting basis set for time-dependent density functional theory calculation of excitation energies: Slater-type orbitals for hydrogen to krypton', *Mol. Phys.* **2005**, *103*, 749–761.
[72] E. van Lenthe, E. J. Baerends, J. G. Snijders, 'Relativistic regular two-component Hamiltonians', *J. Chem. Phys.* **1993**, *99*, 4597–4610.
[73] E. van Lenthe, E. J. Baerends, J. G. Snijders, 'Relativistic total energy using regular approximations', *J. Chem. Phys.* **1994**, *101*, 9783–9792.
[74] E. van Lenthe, J. G. Snijders, E. J. Baerends, 'The zero-order regular approximation for relativistic effects: The effect of spin–orbit coupling in closed shell molecules', *J. Chem. Phys.* **1996**, *105*, 6505–6516.
[75] E. van Lenthe, R. van Leeuwen, E. J. Baerends, J. G. Snijders, 'Relativistic regular two-component Hamiltonians', *Int. J. Quantum Chem.* **1996**, *57*, 281–293.
[76] G. te Velde, F. M. Bickelhaupt, E. J. Baerends, C. Fonseca Guerra, S. J. A. van Gisbergen, J. G. Snijders, T. Ziegler, 'Chemistry with ADF', *J. Comput. Chem.* **2001**, *22*, 931–967.
[77] R. R. Schrock, J. Sancho, S. F. Pederson, S. C. Virgil, R. H. Grubbs, '2,2-Dimethylpropylidyne Tungsten(VI) Complexes

and Precursors for their Syntheses', in 'Inorganic Syntheses', Vol. 26, Ed. H. D. Kaesz, Inorganic Syntheses, Inc., **1989**, pp. 44–51.

[78] S. R. Docherty, N. Phongprueksathat, E. Lam, G. Noh, O. V. Safonova, A. Urakawa, C. Copéret, 'Silica-Supported PdGa Nanoparticles: Metal Synergy for Highly Active and Selective CO_2-to-CH_3OH Hydrogenation', *JACS Au* **2021**, *1*, 450–458.

[79] C. Copéret, A. Comas-Vives, M. P. Conley, D. P. Estes, A. Fedorov, V. Mougel, H. Nagae, F. Núñez-Zarur, P. A. Zhizhko, 'Surface Organometallic and Coordination Chemistry toward Single-Site Heterogeneous Catalysts: Strategies, Methods, Structures, and Activities', *Chem. Rev.* **2016**, *116*, 323–421.

[80] G. R. Fulmer, A. J. M. Miller, N. H. Sherden, H. E. Gottlieb, A. Nudelman, B. M. Stoltz, J. E. Bercaw, K. I. Goldberg, 'NMR Chemical Shifts of Trace Impurities: Common Laboratory Solvents, Organics, and Gases in Deuterated Solvents Relevant to the Organometallic Chemist', *Organometallics* **2010**, *29*, 2176–2179.

[81] D. Massiot, F. Fayon, M. Capron, I. King, S. Le Calvé, B. Alonso, J.-O. Durand, B. Bujoli, Z. Gan, G. Hoatson, 'Modelling one- and two-dimensional solid-state NMR spectra', *Magn. Reson. Chem.* **2002**, *40*, 70–76.

[82] R. R. Schrock, J. D. Fellmann, 'Multiple Metal–Carbon Bonds. 8. Preparation, Characterization, and Mechanism of Formation of the Tantalum and Niobium Neopentylidene Complexes, $M(CH_2CMe_3)_3(CHCMe_3)$', *J. Am. Chem. Soc.* **1978**, *100*, 3359–3370.

[83] J. D. Egbert, S. P. Nolan, 'Tandem deuteration/hydrosilylation reactions catalyzed by a rhodium carbene complex under solvent-free conditions', *Chem. Commun.* **2012**, *48*, 2794–2796.

[84] J. Autschbach, S. Zheng, R. W. Schurko, 'Analysis of electric field gradient tensors at quadrupolar nuclei in common structural motifs', *Concepts Magn. Reson. Part A* **2010**, *36*, 84–126.

[85] P. Pyykkö, 'Year-2017 nuclear quadrupole moments', *Mol. Phys.* **2018**, *116*, 1328–1338.

[86] E. Zurek, C. J. Pickard, J. Autschbach, 'Density Functional Study of the ^{13}C NMR Chemical Shifts in Single-Walled Carbon Nanotubes with Stone–Wales Defects', *J. Phys. Chem. C* **2008**, *112*, 11744–11750.

Received September 26, 2023
Accepted November 23, 2023

